SAMPLING CURVES WITH FINITE RATE OF INNOVATION

Hanjie Pan[1] , Thierry Blu[1] , Pier-Luigi Dragotti[2]

[1]Electronic Engineering
The Chinese University of Hong Kong, Hong Kong
[2]Electrical and Electronic Engineering
Imperial College London, United Kingdom
Emails: {hjpan, tblu}@ee.cuhk.edu.hk, p.dragotti@imperial.ac.uk

ABSTRACT

We focus on a specific class of curves that can be parametrized using a finite number of variables in two dimensions. The corresponding indicator plane, which is a binary image, has infinite bandwidth and can not be sampled and perfectly reconstructed with classical sampling theory. In this paper, we illustrate that it is possible to recover parameters from finite samples of the indicator plane and have a perfect reconstruction of the indicator plane. The algorithm presented here extends the application of FRI signals to multi-dimensional cases and may find its application in field, like super-resolution.

Keywords— Finite rate of innovation, annihilation, sampling, super resolution

1. INTRODUCTION

Sampling plays an essential role in signal processing and data acquisition. Perfect reconstruction from uniform samples for bandlimited signals is guaranteed by Shannon's theory [5], which requires the sampling rate to be at least twice the bandwith of the signal. However, difficulties arise for signals that are infinitely supported in Fourier domain. From Shannon's perspective, such signals cannot be measured precisely in time domain.

A sampling scheme has recently been developed by Vetterli et al. [7] that enables perfect reconstruction from samples of signals that are not bandlimited but that can be parametrized with finite number of variables. Those signals are known to have *finite rate of innovation* (FRI). Examples of such signals are streams of Diracs, piecewise polynomials [2] [7], piecewise sinusoidals [1] for 1-D cases, and 2-D Diracs [4], lines of finite length [4], and polygons [3] [4] [6] for multi-dimensional cases. In this paper, we consider a specific class of parametric curves in two dimensions that have finite degrees of freedom. It can be further generalized to approximate closed simple curves that does not satisfy the parametric model exactly. For noiseless cases, the algorithm achieves perfect reconstruction.

The paper is organized as follows. We first define the curves that can be represented with a few parameters in Section 2. Its relationship with more general curves is also discussed. A closely related concept, interior indicator function, is defined in Section 3 before we start with the sampling scheme in Section 4. Finally, simulation results for the noiseless cases are presented in Section 5.

2. ANNIHILABLE CURVES

We consider a specific class of curves that can be expressed with $K \times L$ complex exponentials with amplitudes $c_{k,l}$:

$$p(x,y) = \sum_{k=1}^{K} \sum_{l=1}^{L} c_{k,l} e^{-j2\pi kx/M - j2\pi ly/N} = 0 \qquad (1)$$

which characterizes curves in an equation form implicitly. The curves defined in (1) are periodic functions with the period $\tau_x = M$ and $\tau_y = N$ along x and y-axis respectively. A closer look at (1) suggests that the coefficients $c_{k,l}$ *annihilate* complex exponentials located at $(\omega_x, \omega_y) = \left(-\frac{2\pi k}{M}, -\frac{2\pi l}{N}\right)$. This is why we denote the curves defined in (1) as "annihilable curves". In principle we would like (1) to characterize a full curve under certain constraints. For instance, if we take the complex conjugate of $p(x,y)$, then the set of equations define another curve. However, we want both the complex conjugate $p^*(x,y)$ and $p(x,y)$ to define the same curve:

$$\sum_{k,l} c_{k,l} e^{-j2\pi kx/M - j2\pi ly/N} = \sum_{k,l} c_{k,l}^* e^{j2\pi kx/M + j2\pi ly/N}$$

$$(2)$$

which corresponds to the Hermitian symmetry requirement of $p(x,y)$. It is equivalent to say $p(x,y)$ is real-valued. We will use this assumption on the curves that interest us throughout this paper. Observe that the curves defined in (1) are completely characterized by its annihilation coefficients $c_{k,l}$. The curves hence belong to a more general category of signals that are known to have *finite rate of innovation* (FRI) [7] [2].

Here comes the question: how is the specific class of curves investigated here related to some very general curves $q(x,y) = 0$, where $q(x,y)$ may not be of the form (1)? It is possible to ap-

proximate it with an annihilable curve by introducing two complex variables: $u = 1 - e^{-j2\pi x/M}$ and $v = 1 - e^{-j2\pi y/N}$, i.e. $x = jM/2\pi \log(1-u)$ and $y = jN/2\pi \log(1-v)$. If we take the Taylor development of $q(jM/2\pi \log(1-u), jN/2\pi \log(1-v))$ around $(u, v) = (0, 0)$, then we are able to approximate the curve with a polynomial in the power of u and v. Hence, the polynomial can be expressed with weighted complex exponentials as in (1), i.e. we find its annihilable curve approximation. The residue between $q(x, y)$ and its annihilable curve approximation is treated as noise which can be easily coped with. Since our primary focus in this paper is on perfect reconstruction from samples, the model mismatch situation is beyond our scope and we will not discuss it here.

3. 2D INDICATOR PLANE

Consider a closed simple curve Γ that contains no holes or loops, the 2D plane is separated into two regions: the interior and exterior of the curve Γ. Define an interior plane indicator function as:

$$\chi_\Gamma(x, y) = \begin{cases} 1 & \text{for } (x, y) \text{ inside } \Gamma \\ 0 & \text{otherwise} \end{cases}$$

which is a binary image with the boundary defined by the curve Γ. Here we do not limit ourselves to specific Γ that satisfies certain properties as long as it is a simple curve. We treat the 2D plane as a complex plane where the (x, y) coordinates correspond to the real part and imaginary part of the complex variable $z = x + jy$ respectively. Then by applying Cauchy's integral formula, the indicator function is equivalent to a line integration along Γ counterclockwise :

$$\chi_\Gamma(x, y) = \frac{1}{2j\pi} \int_\Gamma \frac{\mathrm{d}z_0}{z_0 - x - jy}$$

where $z_0 = x_0 + jy_0$ is the integration variable that corresponds to the point positions along Γ in the complex plane. Another consequence of such interpretation is that we can express the Fourier transform of the indicator plane with an integration of exponential functions:

$$\hat{\chi}_\Gamma(\omega_x, \omega_y) = \frac{1}{\omega_x + j\omega_y} \int_\Gamma e^{-jx_0\omega_x - jy_0\omega_y} \mathrm{d}z_0 \quad (3)$$

which resembles the annihilable curve defined in (1). As we will demonstrate in the following section, such similarity links the annihilable curve with the interior indicator function and plays a key role in the annihilation algorithm.

4. ANNIHILATION OF INDICATOR FUNCTION

Consider an interior indicator function χ_Γ where Γ is the annihilable curve specified in (1), then for any value of ω_x and ω_y,
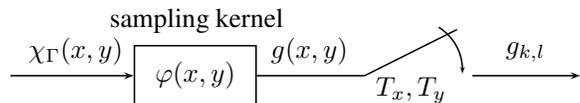
Fig. 1. Sampling of FRI signal

we have:

$$\sum_{k,l} c_{k,l} \left(\omega_x + j\omega_y + \frac{2\pi k}{M} + j\frac{2\pi l}{N} \right) \hat{\chi}_\Gamma \left(\omega_x + \frac{2\pi k}{M}, \omega_y + \frac{2\pi l}{N} \right)$$
$$= \int_\Gamma e^{-jx_0\omega_x - jy_0\omega_y} \underbrace{\sum_{k,l} c_{k,l} e^{-j2\pi kx_0/M - j2\pi ly_0/N}}_{=0 \text{ from } (1)} \mathrm{d}z_0 = 0 \quad (4)$$

It suggests that any $c_{k,l}$ that annihilates the curve Γ is automatically the annihilator of its corresponding interior indicator function. In particular, if we take $\omega_x = -\frac{2\pi k_0}{M}, \omega_y = -\frac{2\pi l_0}{N}$ for $k_0, l_0 \in \mathbb{Z}$, then (4) can be treated as the convolution between the annihilation coefficients $c_{k,l}$ and $h_{k,l}$:

$$c_{k,l} * h_{k,l} = 0 \quad (5)$$

where

$$h_{k,l} = -\left(\frac{2\pi k}{M} + j\frac{2\pi l}{N} \right) \hat{\chi}_\Gamma \left(-\frac{2\pi k}{M}, -\frac{2\pi l}{N} \right) \quad (6)$$

is the annihilation filter. Such equivalence between the indicator plane and its samples is mutual: for a given annihilable curve Γ, its characteristics are completely defined by finite number of samples (which is related to its signal innovation) of the indicator function at discrete grids $\left(-\frac{2\pi k}{M}, -\frac{2\pi l}{N} \right)$ in Fourier domain. Conversely, if enough frequency samples of the indicator function are available, then we can perfectly reconstruct the indicator function, even though the function itself is not bandlimited as is in most cases for FRI signals [1] [2] [4] [6] [7]. The samples contain all necessary information to reconstruct the original function.

Assume the function with period $\tau_x = M$ and $\tau_y = N$ is convolved with a 2D sinc window of bandwidth B_x and B_y, where $B_x\tau_x$, $B_y\tau_y$ are odd integers for the consideration of the convergence of sinc function summation. The signal $g(x, y)$ is then uniformly sampled along both x, y-directions with $T_x = \tau_x/N_x$ and $T_y = \tau_y/N_y$ (Fig 1). Therefore the goal of the algorithm is to reconstruct the annihilable curve Γ, which has $K \times L$ nonzero coefficients $c_{k,l}$, from the $N_x \times N_y$ samples of the indicator plane image:

$$g_{k,l} = \langle \chi(x, y), \mathrm{sinc}(B_x(kT_x - x))\mathrm{sinc}(B_y(lT_y - y)) \rangle$$
$$= \int_0^{\tau_x} \int_0^{\tau_y} \chi(x, y)\varphi(kT_x - x, lT_y - y)\mathrm{d}x\mathrm{d}y \quad (7)$$

where $k = 1, 2, \ldots, N_x, l = 1, 2, \ldots, N_y$ and

$$\varphi(x, y) = \frac{\sin(\pi B_x x) \sin(\pi B_y y)}{B_x B_y \tau_x \tau_y \sin(\pi x/\tau_x) \sin(\pi y/\tau_y)}$$

Algorithm 1: Annihilation of indicator function
1. Compute Fourier transform of the indicator plane χ evaluated at uniformly sampled frequency grids $\left(\frac{2\pi k}{M}, \frac{2\pi l}{N}\right)$;
2. Create annihilation filter according to (6) where the elements are rearranged lexicographically;
3. Solve the annihilation coefficients $c_{k,l}$ based on (5) under the Hermitian symmetry constraint on the coefficients in (2).

is the 2D Dirichlet kernel. The annihilation algorithm is summarized in Algorithm 1.

Thus the annihilation algorithm consists of two key aspects: evaluation of Fourier transform of the indicator plane and retrieval of signal innovation with annihilation filter method.

4.1. Fourier Transform of Indicator Plane

In order to apply the annihilation Algorithm 1, Fourier transform of the annihilable curve Γ has to be evaluated exactly. FRI signals investigated previously in 1-D cases, are either streams of Diracs [7] [2] or piecewise polynomials [1] whose Fourier transform can be computed exactly. However, in the case of annihilable curves here, no explicit expression of the Fourier transform $\hat{\chi}_\Gamma$ is available in general. And we can not use DFT of χ_Γ directly either. Because the indicator plane χ_Γ has infinite bandwith, results obtained from DFT suffers from server aliasing effect. But we can relate the Fourier transform $\hat{\chi}_\Gamma$ with its samples $g_{k,l}$ and calculate the Fourier transform exactly. As is in the case of streams of Diracs [7] [2], we can prove that the Fourier transform coincides with the bandlimited discrete Fourier transform of $g_{k,l}$.

4.2. Retrieval of Signal Innovation

Once the exact Fourier transform $\hat{\chi}$ is evaluated, the annihilating filter is constructed according to (5), from which we can retrieve the coefficients $c_{k,l}$ with annihilation filter method, a well known approach in the reconstruction of FRI signals. Suppose both $c_{k,l}$ and $h_{k,l}$ are rearranged based on the same rule, say column-by-column rearrangement, then (5) is equivalent to a system of equations:

$$\mathbf{HC} = 0 \qquad (8)$$

where $\mathbf{H}$ is a block circulant matrix built from frequency samples of $\hat{\chi}$ and C is the vector that corresponds to $c_{k,l}$ rearranged column-by-column. Thus we can determine the annihilating coefficients uniquely up to a multiplicative constant by solving the linear system of equations (8) for noise-free cases. However, noise is ubiquitous in signal processing, which may arise from the sampling process (Fig 1), the computational inaccuracy as a result of numerical integration in (7), or model mismatch discussed in Section 2 in our case here.

In the presence of noise, the annihilation equation (8) is not satisfied exactly, yet we can still obtain the solution with

(a) Original indicator plane (b) Reconstructed indicator plane

(c) Difference image (d) Samples of indicator plane
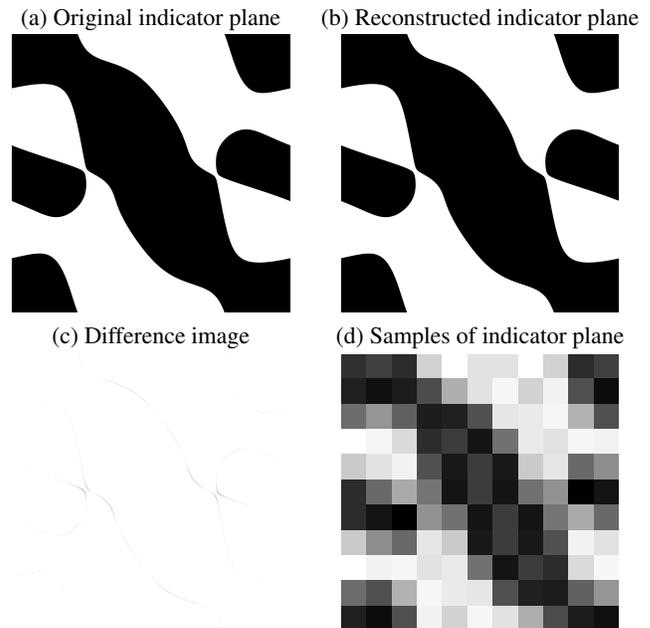
Fig. 2. Annihilation results for noiseless case

the least square approach for the same reasoning as is in 1-D cases [7] [2]. For cases that suffer from more sever noise corruptions, it is better to denoise the samples prior to applying the least square approach with e.g. Cadzow's method [2] for the robustness of the annihilation algorithm against noise perturbation.

Notice that the annihilation algorithm presented here is non-iterative and is extremely fast. Except for the DFT step which is $O(n \log n)$ with the FFT implementation, execution time for all the other steps are linear with KL, the degree of freedom of the annihilable curve. Thus the algorithm can easily cope with large scale problems.

5. SIMULATION RESULTS AND DISCUSSIONS

Several experiments are set up to verify the exact annihilation for noiseless cases. In all the subsequent simulations, we use the same annihilation coefficients $c_{k,l}$, which are 5×5 randomly generated real numbers subject to the Hermitian symmetry constraint in (2). The period of the annihilable curve are chosen to be equal along x, y-axis: $\tau_x = \tau_y = 1$.

Another uncertainty we need to take into account of is the accuracy of numerical integration in (7), which is controlled by the total number of points used for calculation. To avoid ambiguity, we refer to it as "number of numerical integration control points". With less computational accuracy, the samples obtained deviate more from the actual values. The discrepancy can be considered as additive noise. Its effect on the robustness of annihilation algorithm is also investigated in our experiments. To evaluate the relative accuracy, we define the percentile error
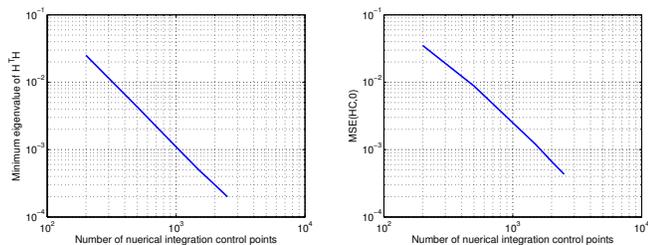
Fig. 3. Robustness of annihilation algorithm

as:

$$\% \text{ error} = \frac{\text{total number of non-zero pixels in error image}}{\text{total number of pixels along curve } \Gamma}$$

5.1. Exact annihilation for noiseless case

For noise-free cases, the algorithm should exactly annihilate the interior indicator function. In simulations, the number of numerical integration control points are 2500×2500 and the samples $g_{k,l}$ are 11×11. Fig 2 are the results obtained from the experiment. The reconstructed indicator plane is almost identical to the original one with the percentile error being 0.3499. Fig 2(c) is the difference between the reconstructed and original indicator plane.

Observe that the samples $g_{k,l}$ and the indicator plane χ_Γ are not displayed to scale. In reality, χ_Γ is $2500/11 \approx 227$ times larger than $g_{k,l}$! Thus the annihilation algorithm investigated here has huge implication for image super-resolution. Such notable results are only possible because we have an exact knowledge on how the signal is modeled (1), which may not be satisfied by general curves in 2-D. But as we have discussed in Section 2, we can have an annihilable curve approximation for any simple closed curve with Taylor development before applying the annihilation algorithm.

Ideally, in the absence of noise, the reconstructed indicator plane should perfectly match the original one. But the algorithm accuracy is limited by the computational error due to numerical integration. Results shown in Fig 3 further support the belief that with increasing number of integration control points, the system is closer to exact annihilation. Here we use both the minimum eigenvalue of $\mathbf{H}^{\mathrm{T}}\mathbf{H}$ and the mean square error (MSE) between annihilation output $\mathbf{H}\mathbf{C}$ and 0 as the measurements.

6. CONCLUSIONS

In this paper, we have shown that particular classes of curves, which are annihilable, can be sampled and perfectly reconstructed. Further we have shown that we can have an annihilable curve approximation for general curves with Taylor expansion. The sampling scheme developed here have many potential applications, including image super resolution, segmentation and data compression.

7. REFERENCES

[1] J. Berent, P.L. Dragotti, and T. Blu. Sampling piecewise sinusoidal signals with finite rate of innovation methods. *Signal Processing, IEEE Transactions on*, 58(2):613–625, 2010.

[2] T. Blu, P. L. Dragotti, M. Vetterli, P. Marziliano, and L. Coulot. Sparse sampling of signal innovations. *IEEE Signal Processing Magazine*, 25(2):31–40, 2008.

[3] I. Maravic and M. Vetterli. A sampling theorem for the Radon transform of finite complexity objects. In *Acoustics, Speech, and Signal Processing, 2002. Proceedings.(ICASSP'02). IEEE International Conference on*, volume 2, pages 1197–1200. IEEE, 2002.

[4] I. Maravic and M. Vetterli. Exact sampling results for some classes of parametric nonbandlimited 2-D signals. *Signal Processing, IEEE Transactions on*, 52(1):175–189, 2005.

[5] Claude E. Shannon. A Mathematical Theory of Communication. *Bell System Technical Journal*, 27:379–423.

[6] P. Shukla and P.L. Dragotti. Sampling schemes for multidimensional signals with finite rate of innovation. *Signal Processing, IEEE Transactions on*, 55(7):3670–3686, 2007.

[7] M. Vetterli, P. Marziliano, and T. Blu. Sampling signals with finite rate of innovation. *Signal Processing, IEEE Transactions on*, 50(6):1417–1428, 2002.